Impact of Gravitational Lensing on Cosmology
Proceedings IAU Symposium No. 225, 2004
Mellier, Y. & Meylan,G. eds.

doi:10.1017/S1743921305001985

Constraints on Dark Energy from Strong Gravitational Lensing by Galaxy Clusters

Massimo Meneghetti[1]†, Carlo Baccigalupi[2], Matthias Bartelmann[1], Klaus Dolag[3], Lauro Moscardini[4], Francesca Perrotta[2], and Giuseppe Tormen[3]

[1]ITA, Universität Heidelberg
[2]SISSA, Trieste
[3]Dipartimento di Astronomia, Università di Padova
[4]Dipartimento di Astronomia, Università di Bologna

Abstract. We discuss two methods for constraining the equation of state of dark energy using strong gravitational lensing by galaxy clusters. In the so called "arc statistics" approach, we compare the cluster efficiency for producing giant arcs in several dark-energy cosmologies and in the "standard" ΛCDM and OCDM models. We find that the expected abundance of gravitational arcs depends on the equation of state of dark energy and reflects the dependence of halo concentrations on cosmology. In agreement with results in previous works, the lensing cross section is very sensitive to dynamical processes occurring in the lenses. Then we use gravitational arcs for tracing the position of the lens critical curves and we measure their scaling with the source redshift in a variety of cosmological models. We find that there is a degeneracy between several lens properties and the equation of state of dark energy which can be broken only after an extremely precise modeling of the lens. Instead of using this "golden lens" approach, we check whether combining the information from a statistical sample of clusters we can distinguish among the various cosmologies. We test the method on a sample of numerically simulated clusters and we reproduce the results expected from the analytic models.

1. Introduction

Evidence is mounting that the Universe is spatially flat, has low matter density and is dominated by some form of dark energy, acting as a repulsive gravitational force and responsible for the present phase of accelerated cosmic expansion (Riess *et al.* 1998, Perlmutter *et al.* 1999, Spergel *et al.* 2003).

Dark energy is thought as a smooth component of the universe with equation of state $p = w(t)\rho c^2$, where ρc^2 is the mean energy density of the universe and the equation of state w assumes negative values in order to produce cosmic acceleration. Theoretical models of dark energy, such as Quintessence scalar fields, predict in general a time variation of the equation of state (see e.g. Peebles & Ratra 2002 and references therein).

We consider here two possible approaches for using strong gravitational lensing by galaxy clusters as a tool for constraining the dark energy equation of state. The first is the "arc statistics" approach. Previous analytic computations and subsequent numerical N-body simulations showed that clusters are characterized by different concentration parameters in different dark energy cosmologies with constant and time-variable equation of state (Dolag *et al.*, 2004). In particular, numerical simulations show that density perturbations grow in a different way in cosmological models with different equation of state of

† Present address: Institut für Teoretische Astrophysik, Tiergartenstr. 15, 69120 Heidelberg, Germany

dark energy, leading to different cluster formation epochs. The concentration reflects the mean value of the density parameter of the Universe when the halo formed. Therefore, halos in dark energy models with equation of state $w > -1$ are found to have concentrations which interpolate between those of corresponding halos in standard ΛCDM and the OCDM models. Since the strong lensing cross section is known to be very sensitive to the lens concentration, we expect large changes in the number of gravitational arcs which clusters in different cosmologies with dark energy are able to produce (Bartelmann *et al.*, 2003).

The second method consists of using multiple gravitational arcs for tracing the position of the lens critical curves for sources at different redshifts. Indeed, the scaling of the critical curves as a function of the source redshift is sensitive to the equation of state of dark energy (Link & Pierce, 1998, Golse, Kneib & Soucail, 2002, Sereno, 2002). A critical issue in the reliability of geometric measurements from cluster lensing is the sensitivity of the results to the mass distribution of the cluster. If the cluster mass were smoothly distributed, then it is easy to see that multiple arcs are a good probe of geometry, but realistic clusters are likely to have substructure and ellipticity. We use here both analytical models and numerical simulations for exploring this problem.

2. Cosmological models and numerical simulations

We consider five cosmological models: an open Cold Dark Matter (OCDM) and four flat dark-energy cosmogonies. The latter are a cosmological constant (ΛCDM) model ($w = -1$), a dark-energy model with constant equation of state (DECDM, $w = -0.6$), and two quintessence models, one with inverse power-law Ratra-Peebles potential (Peebles & Ratra, 2002) (RP) and one with SUGRA potential (Brax & Martin, 2000) (S). The present time value of the equation of state parameter w, describing the ratio between the dark energy pressure and energy density, has been set equal to -0.83 for the RP and S models. For the DECDM, RP, and S models, two sets of simulations were performed by normalizing the power spectrum of the primordial density perturbations either on large scales, with the observed Cosmic Microwave Background (CMB) anisotropies (e.g. Spergel *et al.*), or on small scales, using the observed cluster abundance. In the second case, we choose $\sigma_8 = 0.9$ in all the models.

The results we present here were obtained by making ray-tracing simulations with a sample of 17 dark matter halos. Each of them was simulated in all the previously described cosmologies, building the initial conditions such that the clusters look very similar in all the cosmological models at the present epoch. Full descriptions of the numerical models and of the techniques used in the lensing simulations can be found in Dolag *et al.*(2004) and Meneghetti *et al.* (2000, 2001).

3. The arc statistics approach

3.1. *Lensing cross section*

For each cluster we have measured the lensing cross sections for producing giant arcs, i.e. arcs having a minimum length-to-width ratio L/W. The lensing cross section for any arc property is defined as the area on the source plane where a source must be placed in order to be imaged as an arc characterized by the requested property.

Our results are shown in the left panel of Fig. 1. In the left panel we show the mean cross section of our cluster sample for arcs with length-to-width ratio larger than 7.5 as a function of the cluster redshift.

https://doi.org/10.1017/S1743921305001985 Published online by Cambridge University Press

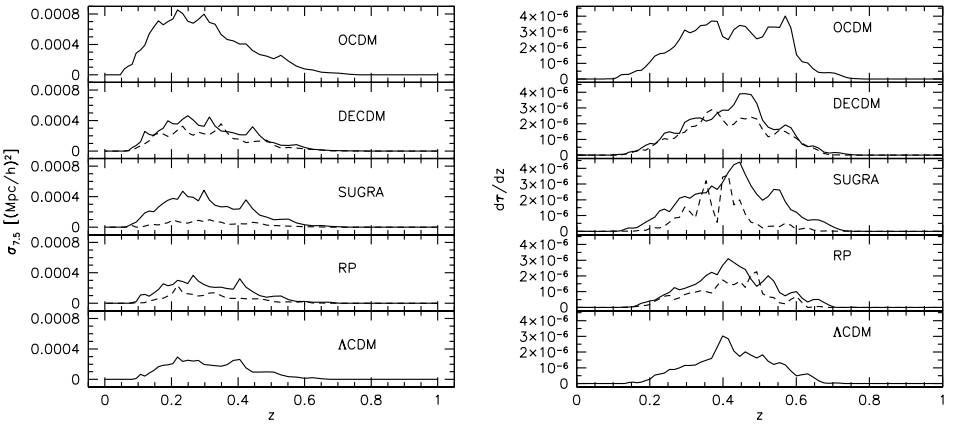

Figure 1. Left panel: averaged lensing cross sections for arcs with length-to-width ratio larger than 7.5 of our cluster sample as function of the lens redshift. Sources are kept at redshift $z_s = 1$. Right panel: differential optical depth for arcs with $L/W > 7.5$ and sources at $z_s = 1$ as a function of the lens redshift. Different panels refer to different cosmological models. Solid curves show the results for cosmologies with $\sigma_8 = 0.9$. Dashed curves show the correspondent results when σ_8 is reduced for taking into account the increasing Sachs-Wolfe effect affecting the large scales in the CMB.

As expected the lensing cross sections reflect the differences in the concentration of dark matter halos in different cosmological models. Assuming the same normalization of the power spectrum, the lensing cross sections for the OCDM and the ΛCDM models differ by roughly a factor of four and the cross sections for the other cosmological models with dark energy interpolate between them. Despite the equation of state of dark energy today is the same for the RP and S models, their lensing cross sections differ significantly at higher redshift.

For models where the CMB normalization of the power spectrum is used, we find mean lensing cross sections smaller by more than one order of magnitude compared to the OCDM model. In fact, when the normalization of the power spectrum derived from the CMB is reduced because of the Integrated Sachs Wolfe (ISW) effect affecting the large scale CMB anisotropies in the cosmologies we consider (Bartelmann *et al.*, 2003), not only the formation epoch of our simulated clusters is delayed, but also their evolution up to redshift zero is changed. For example, clusters in the RP and in the SUGRA models have masses at redshift zero which are smaller by roughly 20% and 30% respectively compared to the ΛCDM model.

The cluster sample is still too small for the mean cross section to be a smooth function of redshift. In fact, the curves exhibit strong peaks which are connected to merger events arising in single clusters. It has been recently shown that during such events, which occur on timescales of some Gyr, the cluster efficiency for strong lensing is strongly enhanced (Torri *et al.*, 2004), due to the combined effect of the increasing shear and convergence. It is interesting to note that, by comparing the cross sections as function of redshift for different cosmological models, there is a correspondence between the number of the peaks in the curves. This is obvious, since we are comparing the same clusters in all cosmological models. However the position and the amplitude of the peaks is strongly dependent on the cosmological model. Indeed the impact of a merger events appear to be larger in cosmologies where halos are less concentrated. Moreover, the different position of the

https://doi.org/10.1017/S1743921305001985 Published online by Cambridge University Press

peaks is produced by the different formation epoch and evolution of clusters, depending on the equation of state of dark energy. The shift of the peaks is more relevant at higher redshift, since our sample is build such to obtain similar objects at redshift $z = 0$ (Dolag *et al.*, 2004).

3.2. *Lensing optical depth*

On the right panel of Fig. 1 we show the differential lensing optical depth for sources at redshift $z_\mathrm{s} = 1$, given by

$$\frac{\mathrm{d}\tau}{\mathrm{d}z} = \frac{1}{4\pi D_\mathrm{s}^2}(1+z)^3 \left|\frac{\mathrm{d}V}{\mathrm{d}z}\right| \int_0^\infty \mathrm{d}M \, \frac{\mathrm{d}n}{\mathrm{d}M}\, \sigma(M,z) \;, \tag{3.1}$$

where D_s is the angular diameter distance to the source plane, V is the cosmic volume, and $\mathrm{d}n(M,z)/\mathrm{d}z$ is the mass function.

The differential optical depth is larger in those cosmological models where lenses form earlier and are thus more concentrated. Moreover, the contribution to the total optical depth comes from clusters in a wider redshift range in these cosmologies. For example, in the high redshift tail, the curves drop to zero at $z \sim 0.65$ and $z \sim 0.8$ in the ΛCDM model and in the OCDM models, respectively. Moreover, at $z \sim 0.6$, the differential optical depth is still close to its maximum in the OCDM model, while it is decreased below 30% in the ΛCDM. Other cosmologies, like the RP, the DECDM and the SUGRA with cluster abundance normalisation, interpolate between these models, while we obtain substantially smaller optical depths by adopting the CMB normalization of the power spectrum.

4. The multiple arcs approach

We discuss now the feasibility of constraining the equation of state dark energy using the observed position of tangential gravitational arcs arising from sources at different redshift. Arcs are strongly distorted images forming around the lens critical line. In the case of an axially symmetric lens, the critical line reduces to the Einstein ring, whose radius depends on the angular diameter distances between the observer and the lens (D_l), the observer and the sources (D_s) and the lens and the source (D_ls) as given by

$$\theta_t = \sqrt{\frac{4GM(\theta_t)}{c^2}\frac{D_\mathrm{ls}}{D_\mathrm{s}D_\mathrm{l}}} \;, \tag{4.1}$$

where $M(\theta_t)$ is the mass enclosed by the Einstein ring and c is the speed of light.

This dependence of the critical line size on geometry can be reversed for constraining the cosmological parameters affecting the angular diameter distances, like the equation of state of dark energy. However, the sensitivity of the results to the mass distribution of the lens represents a critical issue which still has to be accurately investigated.

4.1. *Analytical models*

First, we consider a simple analytic model for describing the lens mass distribution. We use a pseudo-elliptical model, where the ellipticity e is introduced in the lensing potential of a sphere with the Navarro-Frenk-White (NFW) density profile (Navarro, Frenk & White, 1997)

$$\rho(r) = \frac{\rho_s}{(r/r_s)(1+r/r_s)} \;, \tag{4.2}$$

https://doi.org/10.1017/S1743921305001985 Published online by Cambridge University Press

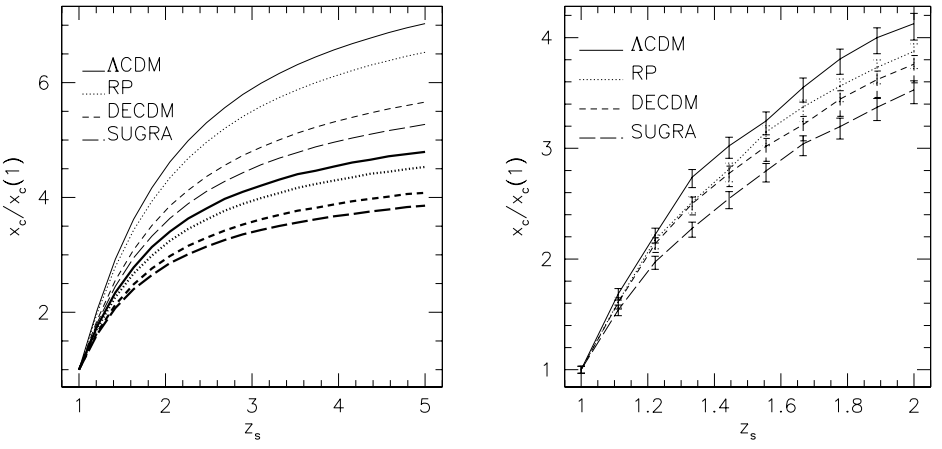

Figure 2. Left panel: sizes of the critical curves for sources at z_s normalized to their value at $z_s = 1$. Results are shown for four cosmological models. The lens mass is $7 \times 10^{14}\ h^{-1} M_\odot$ and the lens redshift is $z_l = 0.6$. The lens is modeled using both an axially symmetric (thin curves) and a pseudo-elliptical (heavy curves) model with NFW density profile. In the elliptical case, the ellipticity of the iso-potential contours is $e = 0.3$.

where r_s and ρ_s are the scale radius and a characteristic density, respectively. The lensing properties of this model are discussed in Meneghetti, Bartelmann & Moscardini (2003) and in Meneghetti *et al.* (2004b).

The expected growth of the critical line size for an halo of mass $M = 7 \times 10^{14}\, h^{-1}\, M_\odot$ at redshift $z_l = 0.6$ as function of the source redshift z_s in a variety of cosmological models is shown in the left panel of Fig. 2 for both the cases of $e = 0$ (thin curves) and $e = 0.3$ (heavy curves). The curves are normalized to the size of the critical curve for sources at $z_s = 1$. The growth of the critical curve with redshift is larger in the ΛCDM model than other cosmologies with dark energy. In this case, for the axially symmetric lens, the growth between $z_s = 1$ and $z_s = 2$ is roughly by a factor of 4.5. Beyond $z_s = 2$, the growth slows down; for sources at $z_s = 5$, critical curves are larger by a factor ~ 7 than for sources at $z_s = 1$. The model which deviates the most from ΛCDM is the SUGRA model, for which the critical curves for $z_s = 2$ and $z_s = 5$ are larger by factors of ~ 3.6 and ~ 5.2, respectively, than for $z_s = 1$. The RP and the DECDM models fall between them.

Adding ellipticity to the model reduces the growth rate of the critical curves for all cosmologies. For $e = 0.3$, the critical curves are larger by a factor of ~ 3.4 for $z_s = 2$ compared to $z_s = 1$ in the ΛCDM model and by a factor of ~ 2.8 in the SUGRA model.

The dependence of the growth rate on the lens ellipticity is due to the steepening of the NFW profile at large radii. In fact, intrinsic ellipticity mimics the effect of an external shear which pushes the lens critical lines at large radii where the density profile is steeper. As shown by Meneghetti *et al.* (2004b), the growth of the critical curves then becomes a shallower function of the source redshift. A similar dependence is found on all the other factors which determine the size of the critical lines for a given source redshift, in particular the lens concentration and redshift.

Since halos of a given mass have different concentration parameters in different cosmologies (see e.g. Dolag *et al.* 2004), a degeneracy between halo mass and cosmology arises in NFW halos. For probing this degeneracy, we carry out the following test. We use an input model consisting of a lens of mass $M = 7.5 \times 10^{14}\, h^{-1}\, M_\odot$ at redshift $z_l = 0.6$

https://doi.org/10.1017/S1743921305001985 Published online by Cambridge University Press

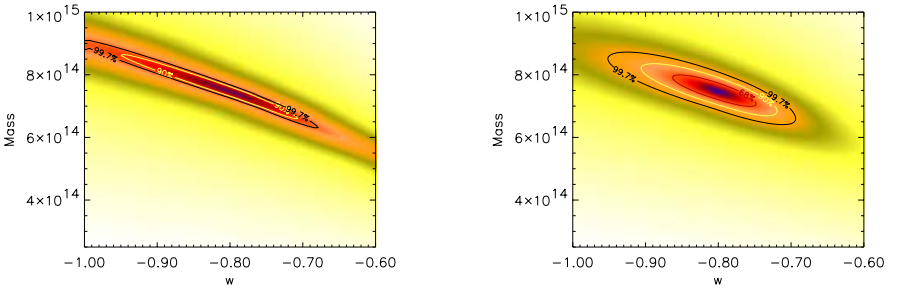

Figure 3. Confidence levels in the w-mass plane. The contours shown by the dark curve correspond to a probability level of 99.7%. The two panels correspond to constraints from two arcs at $z = 1$ and $z = 2$ (left) and from three arcs at $z = 0.8$, $z = 2$ and $z = 3$ plus velocity dispersion at 10 kpc from the center (right).

in a cosmological model with $w = -0.8$. We consider its critical curves for source redshifts $z_s = 1$ and $z_s = 2$, mimicking the constraints from two tangential arcs, and we fit their positions by varying the equation of state of dark energy and the lens mass. For simplicity, we consider only cosmologies with time-independent w. The fit is performed by minimizing

$$\chi_1^2 = \left(\frac{x_1(M,w) - \hat{x}_1}{\Delta_1}\right)^2 + \left(\frac{x_2(M,w) - \hat{x}_2}{\Delta_2}\right)^2 , \tag{4.3}$$

where $\hat{x}_1$ and $\hat{x}_2$ are the positions of the tangential critical curves of the input model for sources at $z_s = 1$ and $z_s = 2$, respectively, Δ_1 and Δ_2 are their respective errors, and $x_1(M,w)$ and $x_2(M,w)$ are the corresponding positions of the critical curves predicted by the fitting model with mass M in a cosmological model with dark-energy equation of state w. We assume here to be in an idealized situation where the location of the critical curves is known at the 1% level.

We show the confidence levels in the w-M plane resulting from this fitting procedure in the left panel of Fig. 3. The innermost and the outermost contours correspond to probability levels of 68% and 99.7%, respectively. As anticipated, a good fit to the position of the critical curves is obtained for a range of M and w, with 99.7 confidence limits ranging between $6 \times 10^{14}\, h^{-1}\, M_\odot \lesssim M \lesssim 9 \times 10^{14}\, h^{-1}\, M_\odot$ and $-1 \lesssim w \lesssim -0.65$.

The degeneracy is hardly broken only if more constraints on the lens density profiles are added. In the right panel of Fig. 3, we show the confidence levels in the w-M plane obtained by using three arcs at $z = 0.8$, $z = 2$ and $z = 3$ plus stellar velocity dispersion data for a simulated cD galaxy in the cluster. To distinguish among different cosmological models becomes easier but does require that we get lucky with the arc redshifts. It is also valid only for the smooth mass distribution represented by our analytical model; real clusters are likely to have a more lumpy structure.

4.2. *Numerical models*

Since asymmetries and substructures play a crucial role in determining the strong lensing properties of galaxy clusters (Meneghetti, Bartelmann & Moscardini, 2003), analytic models can only be used for an approximate description of their lensing properties. More realistic mass distributions of clusters, as provided by numerical simulations, are needed for drawing quantitative conclusions. We now repeat the analysis previously applied to analytic models to a sample of numerical clusters.

https://doi.org/10.1017/S1743921305001985 Published online by Cambridge University Press

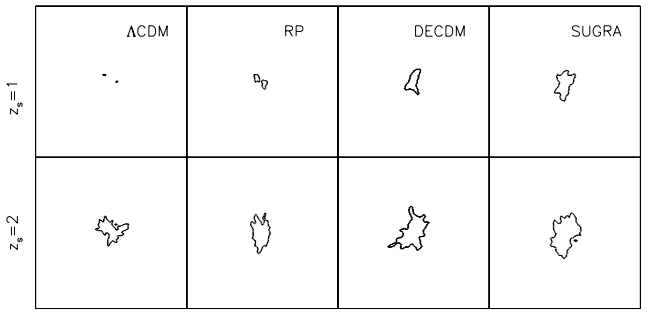

Figure 4. Example showing how the critical curves of a numerical cluster at $z_l = 0.6$ simulated in different cosmological models change between $z_s = 1$ and $z_s = 2$.

The critical curves for one of the clusters in our sample in the different cosmological models are shown in Fig. 4. The sources are at redshift $z_s = 1$ in the upper panels and at $z_s = 2$ in the lower panels. Two important features are evident. First, for sources at redshift z_s the sizes of the critical curves differ substantially among the various cosmological models. For example, the cluster has almost no critical curves in the ΛCDM model, while they are already well developed in the SUGRA model. The RP and the DECDM models fall between these two cosmologies. This is a consequence of the earlier formation epoch of clusters in the RP, DECDM and in the SUGRA models than in the ΛCDM model, due to which they have a larger concentration enabling them to be efficient lenses even at relatively high redshifts or for relatively close sources. Second, as expected from the analytical calculations, the relative enlargement of the critical curves is higher in the ΛCDM than in the other cosmological models.

The right panel of Fig. 2 shows the relative growth of the critical curves in the four cosmological models as measured in the numerical simulations. Each curve represents the median among the 51 halos which develop a critical curve for source redshift $z_s = 1$. The number of useful clusters for this analysis ranges between ~ 20 in the ΛCDM to ~ 30 in the SUGRA model. The results confirm the qualitative expectations from analytic models: namely, the trend for different cosmologies. The absolute values of the relative growth are also consistent with the predictions for a moderate ellipticity ($e \lesssim 0.3$) lensing potential (compare the two panels of Fig. 2).

These results show that the statistical application of this method is potentially powerful. Upcoming surveys from space, like those which will be conducted by SNAP (Aldering *et al.*, 2004), could provide detailed observations of order thousand galaxy clusters, allowing the information from many lenses to be combined. The error bars in Fig. 2 show the first and the third quartiles of the curve distribution we obtain from our numerical cluster sample. They were rescaled to the expected error when the information from ~ 1000 pairs of arcs is combined. The figure shows that when constraints on the position of the critical curves from sources at significantly different redshifts and in a sufficiently large sample of clusters are used, it becomes possible to discriminate among different cosmological models. We have used a simple choice of source redshifts; by extending the analysis to a wider redshift range, especially to redshifts beyond 2 for the distant arcs, the constraints became stronger. The analysis needs to be extended in other ways as well, by combining the information from different lens redshifts and finding the best way to weight a given cluster.

https://doi.org/10.1017/S1743921305001985 Published online by Cambridge University Press

5. Summary and discussion

We have explored two methods for constraining the equation of state of dark energy.

The first is based on arc statistics: different abundances of long and thin arcs are expected on the sky in different cosmologies. Using numerically simulated galaxy clusters we find that dark energy cosmologies interpolate between ΛCDM and OCDM models. The dependence of the abundance of long and thin arcs on the dark energy equation of state reflect the sensitivity of halo concentrations on w shown in earlier papers. The lensing cross sections result to be very sensitive to merger events occurring in the clusters. This suggests that arc statistics can be a very powerful tool for probing the structure formation.

Then, we make an exploratory study of how well dark energy models can be constrained using lensed arcs at different redshifts behind cluster lenses. We quantify the sensitivity to lens mass, concentration and ellipticity with analytical models that include the effects of dark energy on halo structure. We show that degeneracies between mass models and cosmography may be broken only using additional constraints on the lens density profile. However we conclude that the requirements on the data are so stringent that it is very unlikely that robust constraints can be obtained from individual clusters. We argue that surveys of clusters, analyzed in conjunction with numerical simulations, are a more promising prospect for arc-cosmography. We use numerically simulated clusters to estimate how large a sample of clusters/arcs could provide interesting constraints on dark energy models. We focus on the scatter produced by differences in the mass distribution of individual clusters. We find from our sample of simulated clusters that at least 1000 pairs of arcs are needed to obtain constraints if the mass distribution of individual clusters is taken to be undetermined.

References

Aldering, S. C. G., *et al.* 2004, ArXiv Astrophysics e-prints, astro-ph/0405232
Bartelmann, M., Meneghetti, M., Perrotta, F., Baccigalupi, C., & Moscardini, L. 2003, A&A, 409, 449
Brax, P., Martin, J., 2000, PRD, 61, 103502
Dolag, K., Bartelmann, M., Perrotta, F., Baccigalupi, C., Moscardini, L., Meneghetti, M., & Tormen, G. 2004, A&A, 416, 853
Golse, G., Kneib, J.-P., & Soucail, G. 2002, A&A, 387, 788
Meneghetti, M., Bolzonella, M., Bartelmann, M., Moscardini, L., & Tormen, G. 2000, MNRAS, 314, 338
Meneghetti, M., Yoshida, N., Bartelmann, M., Moscardini, L., Springel, V., Tormen, G., & White, S. D. M. 2001, MNRAS, 325, 435
Meneghetti, M., Bartelmann, M., & Moscardini, L. 2003, MNRAS, 340, 105
Meneghetti, M., Bartelmann, M., Dolag, K., Moscardini, L., Perrotta, F., Baccigalupi, C., & Tormen, G. 2004a, ArXiv Astrophysics e-prints, astro-ph/0405070
Meneghetti, M., Jain, B., Bartelmann, M., & Dolag, K. 2004b, ArXiv Astrophysics e-prints, astro-ph/0409030
Navarro, J, Frenk, C., White, S., 1997, ApJ, 490, 493
Peebles, P., Ratra, B., 2002, Rev. Mod. Phys., 75, 599
Perlmutter, S., *et al.* 1999, ApJ, 517, 565
Riess, A. G., *et al.* 1998, AJ, 116, 1009
Sereno, M. 2002, A&A, 393, 757
Soucail, G., Kneib, J.-P., & Golse, G. 2004, A&A, 417, L33
Spergel, D. N., *et al.* 2003, ApJS, 148, 175
Torri, E., Meneghetti, M., Bartelmann, M., Moscardini, L., Rasia, E., & Tormen, G. 2004, MNRAS, 349, 476